CHEMISTRY OF MATERIALS
Cite This: Chem. Mater. 2019, 31, 179−189
Article
pubs.acs.org/cm

General Principle for Fabricating Natural Globular Protein-Based Double-Network Hydrogels with Integrated Highly Mechanical Properties and Surface Adhesion on Solid Surfaces

Ziqing Tang,[†] Qiang Chen,*[,†] Feng Chen,[†] Lin Zhu,[†] Shaoping Lu,[†] Baiping Ren,[‡] Yanxian Zhang,[‡] Jia Yang,[†] and Jie Zheng*[,‡]

[†]School of Materials Science and Engineering, Henan Polytechnic University, Jiaozuo 454003, China
[‡]Department of Chemical and Biomolecular Engineering, The University of Akron, Akron, Ohio 44325, United States

Supporting Information

ABSTRACT: Developing functional hybrids of globular proteins and synthetic polymers into multipurpose tough hydrogels remains challenging. Here, we propose a new strategy combining double-network and protein misfolding concepts to create diverse protein−polymer double-network (DN) hydrogels with both high bulk and interfacial toughness. The method integrates an intrinsic heat-induced protein denaturation/aggregation feature and a double-network concept, which produces different bovine serum albumin (BSA)-based DN hydrogels with hybrid physical−chemical cross-linking or fully physical cross-linking to achieve a high modulus of 252−1199 kPa, high strength of 0.24−0.48 MPa, high fracture energy of 3.56−16.88 MJ/m^3, high extensibility of 7.7−79.9 mm/mm, fast self-recovery (stiffness/toughness recovery of 94/80% after heat treatment at 80 °C for 30 min), and strong surface adhesion to various nonporous solid surfaces (interfacial toughness of 1176−2827 J/m^2). Such tough and adhesive protein−polymer hydrogels have great potential for different applications, such as artificial soft tissues, flexible electronics, and wearable devices.

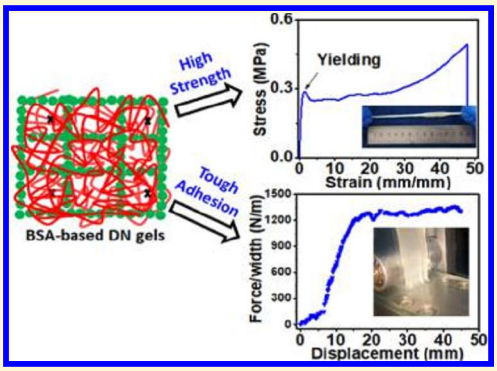

1. INTRODUCTION

Polymer hydrogels have been well developed, studied, and used in many fundamental research and practical applications,[1−7] including drug delivery carriers, soft actuators, tissue engineering, and contact lenses, due to their abundant functional groups, the simplicity and diversity of synthesis methods, a wide availability of raw materials, and cost-effective production.[8−10] However, less attention has been given, and less progress made to develop hydrogels made of natural biomolecules (i.e., proteins and peptides).[11−13] In particular, use of natural proteins as basic building blocks to construct a gel network allows to deliver several intrinsic advantages, including excellent biocompatibility/biodegradability and low cell toxicity/immune response.[12,14] Several protein-based hydrogels have been developed using fibrous proteins (e.g., collagen, keratin, elastin, and silk fibroin (SF))[15,16] and globular proteins (e.g., β-lactoglobulin, serum albumin, casein, and ovalbumin (OVA)).[17] However, almost all of these protein-based hydrogels experience weak mechanical properties, as evidenced by tensile stress of 100−300 kPa. To improve mechanical properties of protein-based hydrogels, a common strategy is to incorporate different fillers and cross-linkers (nanocomposites, surfactants, and polymers) with proteins to form a hybrid simple- or single-network (SN) structure.[18−20] But, such mechanical improvement in most cases is rather limited and far below that of those "strong" hydrogels with tensile stress of 1 MPa and tensile strain >1000%. For instance, the incorporation of laponite nanoclay or reduced graphene oxide (rGO) into natural gelatin-based hydrogels allows to improve their storage modulus (G') to 1.5 kPa for laponite nanoclay−gelatin hydrogels,[21] compressive modulus to 12.9 kPa for laponite nanoclay−gelatin methacrylate hydrogels,[22] and Young's modulus to 22.5 kPa for rGO−gelatin methacrylate hydrogels,[23] respectively. Silk fibroin (SF)-incorporated cryogels with a single-network, a double-network (DN), and a triple network structure demonstrated their compressive strengths of 1−3, 87, and 240 MPa, as well as compressive modulus of 48, 66, and 126 MPa,[24] respectively. However, no tensile tests were reported in these SF cryogels. In addition, regenerated silk fibroin hydrogels mixed with hydroxypropyl methyl cellulose or sodium dodecyl sulfate could achieve tensile strength of 0.4 or 0.7 MPa;[25,26] collagen−poly(ethylene glycol) (PEG) hydrogels achieved tensile stress−strain of 27.1 kPa/318%, much higher than that of 7.07 kPa/36% for PEG hydrogels;[27] casein/polyacrylamide (casein/PAAm) hydrogels showed high toughness/stretchability of 3000 J/m^2/3500%.[28] Although these conventional strategies have institutively improved

Received: September 11, 2018
Revised: December 5, 2018
Published: December 6, 2018

DOI: 10.1021/acs.chemmater.8b03860
Chem. Mater. 2019, 31, 179−189

Scheme 1. (a) Scheme of Preparation of BSA/PAAm DN Gels via a One-Pot Heating-Photopolymerization Method; (b) Structure of Monomers Used for the Second Network and the Formation of the First Physical BSA Network via Heat-Induced Globular Protein Denaturation and Gelation Process

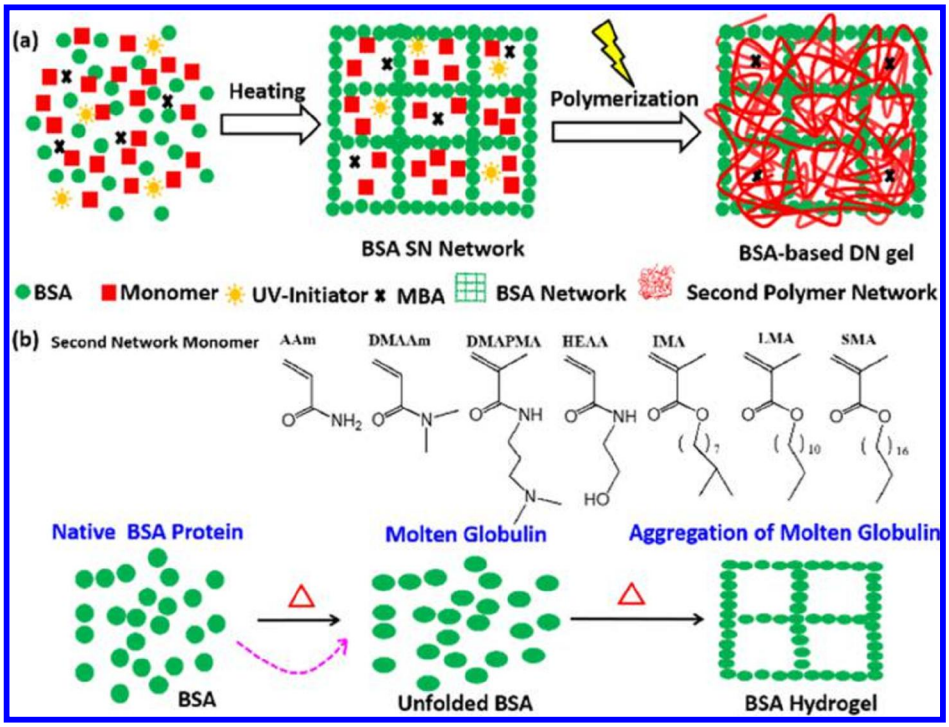

mechanical properties of the protein-based hydrogels to some extent, the existing strategies and the protein-based hydrogel systems still have some limitations: (i) Simple incorporation of different proteins into different hydrogel networks via copolymerization or physical blending does not provide a general or fundamental solution to protein-based hydrogels with high mechanical properties. (ii) Most protein-based hydrogels are based on fibrous protein, not globular proteins, presumably because fibrous proteins could self-assemble into nanostructures with similar morphologies to natural soft tissues.

More importantly, many natural proteins (e.g., mussels, barnacles, and slugs) secreted by living organisms are able to strongly adhere to virtually all soft and hard surfaces regardless of their surface properties.[29,30] So, it is intuitive to design adhesive hydrogels by incorporating these natural proteins into gel network.[31] As expected, although mussel-inspired hydrogels, the most commonly used adhesive hydrogels, show a general surface adhesion to a variety of solids, surface adhesion is very weak (10^1–10^2 kPa).[32] Moreover, mussel-inspired adhesive hydrogels usually contain catechol-containing groups, which are very easily oxidized, leading to the loss of surface adhesion. The relatively weak adhesion of protein-based hydrogels could be attributed to the weak mechanical strength of bulk hydrogels,[33] because the design of a strong and tough hydrogel–solid interface generally requires high fracture toughness of the hydrogel itself. Most hydrogels still possess either property, i.e., most adhesive hydrogels are not tough and strong hydrogels and vice versa.[34–39]

Different from weak protein-based adhesives, three double-network polymer hydrogels poly(2-acrylamido-2-methyl-1-propane sulfonic acid) (PAMPS)/PAAm,[40] alginate/PAAm,[41,42] and agar/poly(*N*-(2-hydroxyethyl)acrylamide) (PHEAA)[43] are reported as the toughest adhesive hydrogels in the literature. All three polymer hydrogels can achieve high bulk toughness (1–5 MPa of tensile stress and 1000 J/m^2 of fracture energy) and high interfacial toughness (1000 J/m^2 for PAMPS/PAAm, 1000–1750 J/m^2 for alginate/PAAm, and 2000–5600 J/m^2 for our agar/PHEAA). The two former hydrogels require a special treatment of substrates (either surface modification or porous structure) to realize high interfacial toughness; i.e., PAMPS/PAAm hydrogels[40] achieve high interfacial toughness by anchoring polymer chains inside porous solid substrates, whereas alginate/PAAm hydrogels achieve high interfacial toughness by chemically anchoring the long-chain polymers onto nonporous solid surfaces via silane or 1-ethyl-3-(-3-dimethylaminopropyl)carbodiimide hydrochloride.[41] Agar/PHEAA hydrogels with fully physically cross-linked networks achieved high interfacial toughness at different nonporous solid substrates without any surface treatment.[43]

Inspired by the "double-network" design of polymer hydrogels above with both strong interfacial and bulk toughness, only a few natural fibrous protein-based hydrogels have been fabricated with double-network (DN) structures,[24,28,44–46] not considering globular protein-based hydrogels. None of the existing protein-based hydrogels have demonstrated both interfacial and bulk toughness simultaneously. To fill this gap, here, we propose to apply a "double network" and "protein misfolding" principle to fabricate natural globular protein–synthetic polymer hydrogels with both excellent surface adhesion and mechanical properties using a simple two-step procedure. Bovine serum albumin (BSA) is selected as a model protein because BSA is a typical natural globular protein with high water solubility, ease of gelation, biocompatibility, and low production cost.[47,48] Our BSA-based

DOI: 10.1021/acs.chemmater.8b03860
Chem. Mater. 2019, 31, 179–189

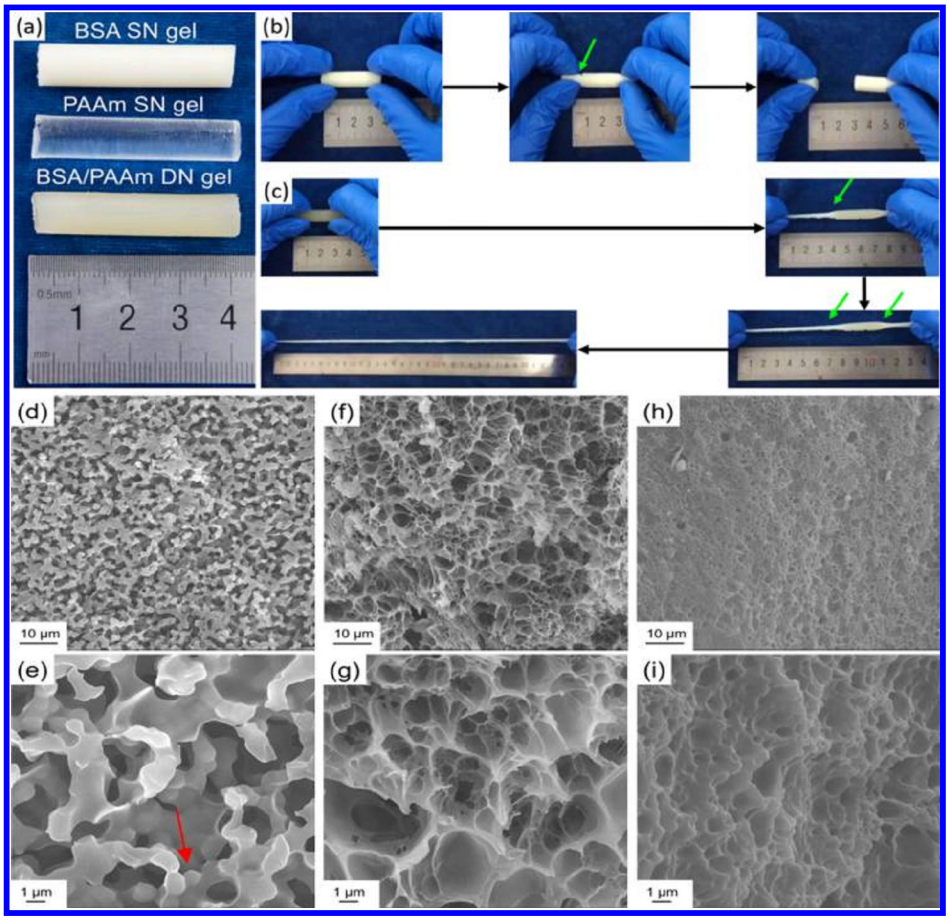

Figure 1. (a) Appearance of BSA SN gel, PAAm SN gel, and BSA/PAAm DN gel; tensile stretching for (b) BSA SN gel and (c) BSA/PAAm DN gel; and scanning electron microscopy images for the network structures of BSA SN gel (d, e), PAAm SN gel (f, g), and BSA/PAAm DN gel (h, i) at different resolutions.

DN hydrogels exhibit not only a high compressive strength of 50 MPa and high tensile strength of 0.48 MPa but also tough interfacial bonding to various nonporous solids without any surface modification (interfacial toughness of 1176−2827 J/m^2). We believe our design strategy and BSA-based DN gels will open a new avenue to develop hybrid protein−polymer hydrogels and explore different applications.

2. RESULTS AND DISCUSSION

As shown in Scheme 1a,b, all reactants, including BSA, the second-network monomers (i.e., acrylamide (AAm), *N*,*N*′-dimethylacrylamide (DMAAm), *N*-(3-dimethylaminopropyl)-methacrylamide (DMAPMA), *N*-(2-hydroxyethyl)acrylamide (HEAA), isodecyl methacrylate (IMA), lauryl methacrylate (LMA), or stearyl methacrylate (SMA)), UV-initiators, and chemical cross-linker (*N*,*N*′-methylenebis(acrylamide) (MBA)), were dissolved in water at room temperature (R.T.) to obtain a transparent light-yellow precursor solution. Then, the precursor solution was heated up to at 80 °C for 10 min to form the first BSA network, during which the heating temperature (>60 °C) led to the unfolding of BSA to adopt molten globulin conformation at the expense of its α-helix content.[49,50] The heating-induced unfolding of BSA proteins also caused the exposure of their buried hydrophobic groups to increase the noncovalent interactions that lead to the aggregation of these unfolded BSA proteins to form the first network (Scheme 1b).[50] Meanwhile, during the heating process, the precursor of the second network (e.g., second-network monomers, UV-initiators, and chemical cross-linkers if any) was inert and embedded in the BSA network so that in the second step of photopolymerization, the ductile synthetic network was formed and interpenetrated with the BSA network. The resulting BSA/polymer DN gels, consisting of the first physical BSA network and the second either covalent (PAAm, poly(*N*,*N*′-dimethylacrylamide) (PDMAAm) or P(AAm-*co*-DMAPMA)) or noncovalent (PHEAA, P(AAm-*co*-IMA), P(AAm-*co*-LMA), or P(AAm-*co*-SMA)) network, possess either a hybrid cross-linked or a fully physically linked DN structure. Different from the aforementioned protein-based hydrogels, in our strategy, the globular protein needs to be denatured and gelated by heating (like egg cooking) and the protein gel needs to be strong enough to act as a sacrificial network for effective energy dissipation. The presence of rich $-NH_2$, −COOH, or −OH groups in BSA proteins also allows to form intensive physical or chemical interactions between BSA−polymer networks and between the networks and substrates, wherein the reversible physical interactions would offer reversible self-recovery of the networks.

Figure 1 shows a side-by-side comparison of appearance, stretching, and microstructure among BSA single-network (SN) gel, PAAm SN gel, and BSA/PAAm DN gel. BSA SN gel was milk white, easily breaking when stretched, and formed a random aggregated network (red arrows) due to the heat-

DOI: 10.1021/acs.chemmater.8b03860
Chem. Mater. 2019, 31, 179−189

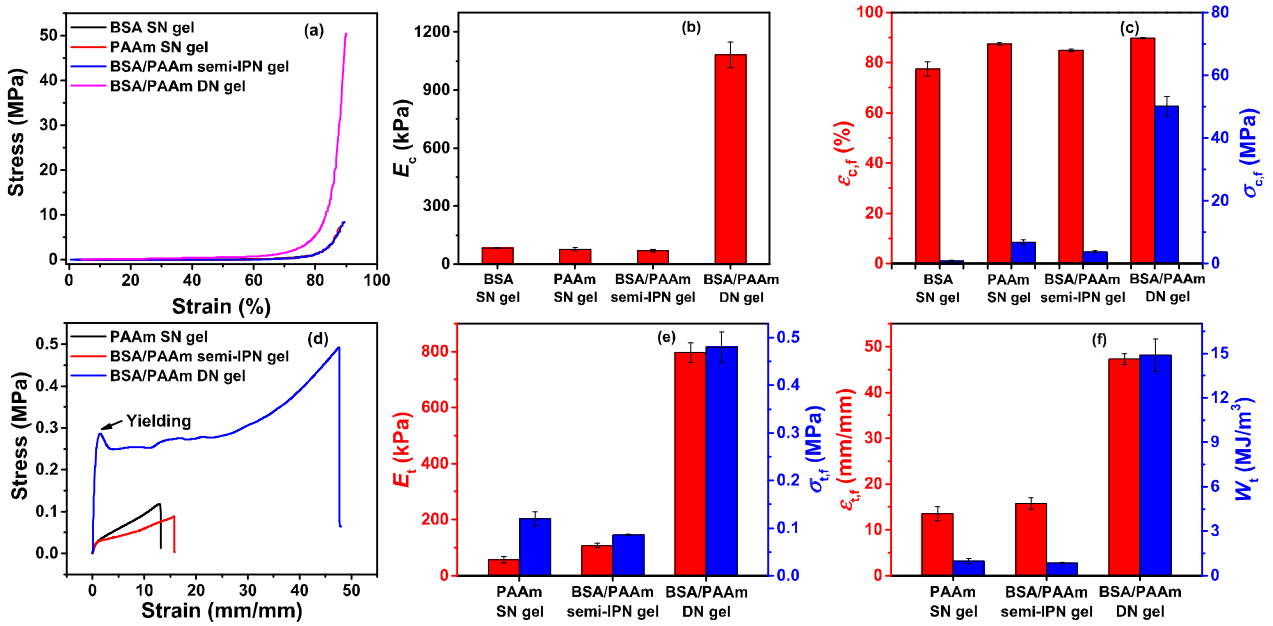

Figure 2. (a) Compression stress−stain curves of BSA SN gel, PAAm SN gel, BSA/PAAm semi-IPN gel, and BSA/PAAm DN gel and the corresponding (b) elastic modulus and (c) fracture strain and stress. (d) Tensile stress−strain curves of PAAm SN gel, BSA/PAAm semi-IPN gel, and BSA/PAAm DN gel and the corresponding (e) elastic modulus and fracture stress and (f) fracture strain and work of extension.

induced structural denaturation and aggregation of unfolded BSA proteins (Figure 1a,b,d,e). PAAm SN gel showed a transparent appearance, with loosely formed pore structures, the larger pore sizes being 2−8 μm, and a wide pore size distribution (Figure 1a,f,g). Different from either SN gels, the opaque BSA/PAAm DN gel exhibited a much denser pore structure with a relatively uniform pore size of ∼1 μm (Figure 1h,i). This indicates that the aggregated BSA proteins not only provide a stronger structural integrity to the DN structure but also enhance their hydrophobic interactions and hydrogen bonding between and within both networks upon heat-induced structural denaturation. As a result, BSA/PAAm DN gel can be stretched to 7.5 times its initial length without breakage, during which the necking phenomenon was clearly observed (Figure 1c).

The structural enhancement features of BSA/PAAm DN gels are further quantified by the compressive and tensile tests. As shown in Figure 2a−c, BSA/PAAm DN gel (compressive stress/compressive strain/compressive modulus = 50 MPa/89.8%/1082 kPa) demonstrated much better compressive properties than those of BSA SN gel (1.05 MPa/77.5%/84 kPa), PAAm SN gel (6.81 MPa/87.5%/76 kPa), and BSA/PAAm semi-IPN gel (3.73 MPa/84.9%/68 kPa). For even more challenging tensile tests, BSA/PAAm DN gel achieved a high tensile modulus (E_t)/fracture stress ($\sigma_{t,f}$) of 795.5 kPa/0.48 MPa, which was 7.4/13.9 times stiffer and 5.6/4 times stronger than that of BSA/PAAm semi-IPN gel (E_t of 108.1 kPa, $\sigma_{t,f}$ of 0.086 MPa) and PAAm SN gel (E_t of 57.3 kPa, $\sigma_{t,f}$ of 0.12 MPa) (Figure 2d,e). BSA SN gel was too brittle for tensile tests. Moreover, BSA/PAAm DN gel reached a fracture strain ($\varepsilon_{t,f}$) of 47.30 mm/mm and work of extension (W), 14.88 MJ/m^3, which were still much higher than those of BSA/PAAm semi-IPN gel ($\varepsilon_{t,f}$ of 15.78 mm/mm, W of 0.85 MJ/m^3) and PAAm SN gel ($\varepsilon_{t,f}$ of 13.51 mm/mm, W of 0.99 MJ/m^3) (Figure 2f). In addition, the tensile stress−strain curves also showed a distinct yielding behavior of BSA/PAAm DN gel (Figure 2d), consistent with the necking phenomenon in Figure 1c. It is also interesting to observe that without heating, the simple incorporation of native BSA proteins into PAAm gel (namely, BSA/PAAm semi-IPN gel) led to an adverse effect on both compressive and tensile properties so that BSA/PAAm semi-IPN gel showed even weaker mechanical properties than those of PAAm SN gel. This is probably because without heating, BSA proteins in the PAAm network will largely retain their native structure and unaggregated state; upon photopolymerization of AAm, free $-NH_2$ and $-SH$ groups in BSA would serve as chain-transfer sites, leading to weaker mechanical properties. In contrast, upon heating, denatured and aggregated BSA would form a brittle physical gel, which can act as the first network of DN gels to dissipate energy during deformation. Thus, BSA/PAAm DN hydrogels with both high strength and toughness can be obtained through a simple heating-induced protein denaturation and aggregation process without the requirement of additional components/cross-linkers or chemical modifications of BSA.

To gain additional insight into the reinforcement mechanism of hybrid DN hydrogels, we prepared BSA/PAAm DN gels under widely varied fabrication conditions and performed a series of tensile tests to examine the effects of BSA concentration (C_{BSA}), AAm concentration (C_{AAm}), heating temperature, and heating time on the mechanical properties of BSA/PAAm DN gels and results are summarized in Figure S1 and Tables S1−S4. In Figure S1a and Table S1, as C_{BSA} < 300 mg/mL, BSA/PAAm DN gels showed very weak tensile properties ($\sigma_{t,f}$ = 0.087−0.123 MPa), presumably because C_{BSA} was too low to serve as "sacrificial bonds" and to form a sufficiently strong protein network. As C_{BSA} = 500 mg/mL, BSA/PAAm DN gels significantly improved their fracture stress to 0.48 MPa at a fracture strain of 47.3 mm/mm, which were 4−5 times greater than those of the gels prepared at C_{BSA} < 300 mg/mL. Both yielding and necking phenomenon were observed, confirming that a strong BSA network was formed to

DOI: 10.1021/acs.chemmater.8b03860
Chem. Mater. 2019, 31, 179−189

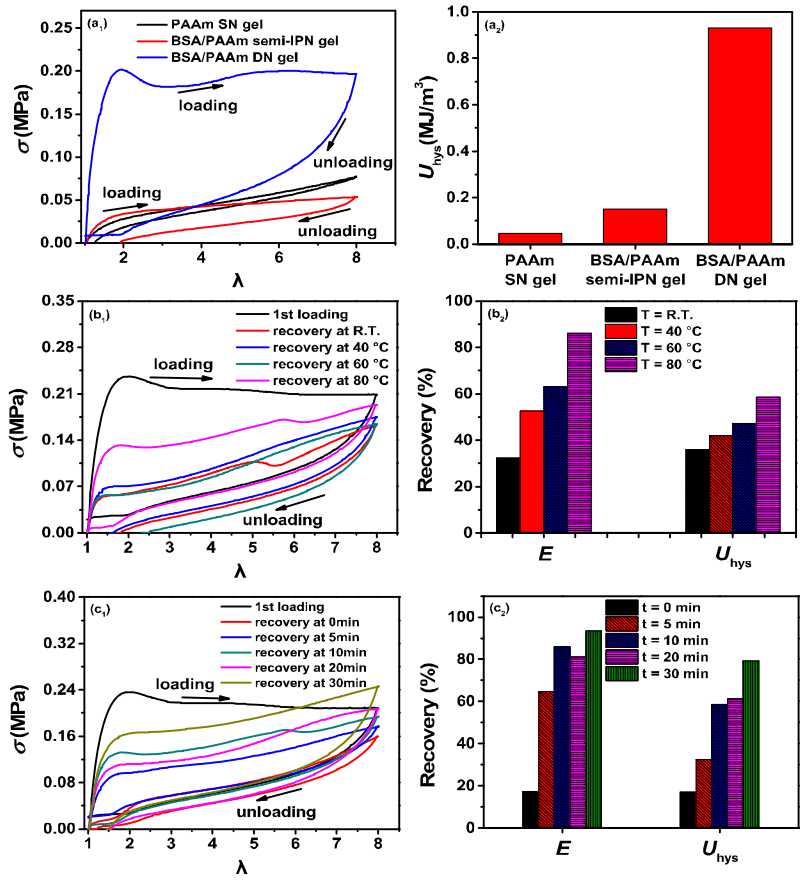

Figure 3. (a) Cyclic loading–unloading curves and the corresponding dissipated energies of BSA SN gel, BSA/PAAm semi-IPN gel, and BSA/PAAm DN gel at $\lambda = 8$. (b) Temperature-dependent mechanical and self-recovery properties of BSA/PAAm DN gels at $\lambda = 8$ with heating time of 10 min. (c) Resting time-dependent mechanical and self-recovery properties of BSA/PAAm DN gels at $\lambda = 8$ with heating temperature of 80 °C.

bear stress and dissipate energy before the fracture of the second covalent PAAm network. Moreover, BSA/PAAm DN gels reached the best tensile properties (E_t of 759.5 kPa, σ_f of 0.478 MPa; ε_f of 47.3 mm/mm, and W of 14.88 MJ/m^3) at AAm = 30% (Figure S1b and Table S2). The heating procedure is also critical for the BSA network formation. In Figure S1c and Table S3, at T = 50 °C, BSA/PAAm DN gel showed a weak fracture stress of 0.22 MPa at a large strain of 34.7 mm/mm without the yielding point being observed. Increase of the heating temperature to ≥60 °C led to the appearance of yielding points and much stronger mechanical properties for all BSA/PAAm DN gels. Particularly, at T = 80 °C, BSA/PAAm DN gel reached a maximal fracture stress of 0.48 MPa at strain of 47.3 mm/mm. Moreover, the increase of heating time to an optimal value of 10 min at 80 °C can further improve tensile stress–strain to 0.48 MPa/47.3 mm/mm (Figure S1d and Table S4). These results indicated that heating temperatures of >60 °C and heating time of ∼10 min are critical parameters to form a strong BSA network through the denaturation and aggregation of BSA proteins, which serve as sacrificial bonds to strengthen the covalent PAAm network. Unless otherwise stated, we mainly used BSA/PAAm DN gels prepared at the optimal conditions (C_{BSA} of 500 mg/mL, C_{AAm} of 30% w/v, heating time of 10 min, and heating temperature of 80 °C) for tests.

Cyclic loading–unloading experiments were performed to quantitatively evaluate the energy dissipation mode of BSA/PAAm DN gels. Compared to PAAm SN gel and BSA/PAAm semi-IPN gel, BSA/PAAm DN gel displayed a significantly large hysteresis loop with a yielding point (Figure 3a$_1$). Accordingly, at the same strain of 8, the dissipated energies (U_{hys}) of BSA/PAAm DN gel were 0.93 MJ/m^3, which were 20.7 and 6.2 times larger than those of PAAm SN gel (0.045 MJ/m^3) and BSA/PAAm semi-IPN gel (0.150 MJ/m^3) (Figure 3a$_2$). In comparison, BSA/PAAm semi-IPN gel, without forming a BSA network in the gel, displayed a much smaller hysteresis loop, indicating that the presence of the BSA network serves as sacrificial bonds to dissipate large energy during the deformation. Furthermore, cyclic loading tests were also performed on different fresh DN gels at different maximum strains (λ_{max}) and at different stretching rates. Evidently, hysteresis loop areas increased with λ_{max} from a small hysteresis loop (U_{hys} of 0.11 MJ/m^3) at λ_{max} = 2 to the large loop (U_{hys} of 2.5 MJ/m^3) at λ_{max} = 20 (Figure S2a and Table S5), as well as increased from 0.82 to 1.01 MJ/m^3 as the stretching rate increased from 5 to 500 mm/min (Figure S2b and Table S6), showing the dependence of the stretching rate and tensile strain on energy dissipation. Because of the physical nature of the BSA network, we further examined both elastic modulus-based (stiffness) self-recovery and dissipated energy-based (toughness) self-recovery of BSA/PAAm DN gels in response to heating temperature and heating time after the first loading–unloading. As shown in Figure 3b$_1$, the hysteresis loops became larger after the gels were recovered at the higher temperatures. The stiffness/toughness recovery of the BSA/PAAm DN gels was 53/42% at 40 °C, 63/47% at 60 °C, and

DOI: 10.1021/acs.chemmater.8b03860
Chem. Mater. 2019, 31, 179–189

Table 1. Tensile Properties of Different Protein-Based DN Gels[a]

DN gels	E (kPa)	ε_f (mm/mm)	σ_f (MPa)	W (MJ/m^3)
BSA_{500}–$PAAm_{30}$[b]	795.50 ± 35.14	47.30 ± 1.16	0.48 ± 0.032	14.88 ± 1.09
BSA_{500}–$PDMAAm_{30}$[b]	1199.00 ± 41.01	7.71 ± 0.08	0.31 ± 0.007	2.64 ± 0.038
BSA_{500}–$P(DMAPMA_5$-*co*-$AAm)_{30}$[b]	251.67 ± 15.56	35.90 ± 0.61	0.33 ± 0.021	7.39 ± 0.32
BSA_{500}–$PHEAA_{50}$[c]	569.33 ± 88.57	9.19 ± 0.64	0.34 ± 0.035	3.56 ± 0.48
BSA_{500}–$P(IMA_1$-*co*-$AAm)_{30}$[c]	620.67 ± 69.92	79.90 ± 5.53	0.25 ± 0.026	16.88 ± 1.24
BSA_{500}–$P(LMA_1$-*co*-$AAm)_{30}$[c]	637.00 ± 7.07	71.54 ± 0.70	0.24 ± 0.014	15.73 ± 0.65
BSA_{500}–$P(SMA_1$-*co*-$AAm)_{30}$[c]	467.00 ± 104.55	78.42 ± 2.31	0.24 ± 0.007	14.90 ± 1.21
OVA_{100}–$PDMAAm_{30}$[b]	11.70 ± 1.12	7.84 ± 0.80	0.052 ± 0.004	0.28 ± 0.049

[a]BSA_x–PM_z or BSA_x–$P(M_y$-*co*-$AAm)_z$: x is BSA concentration (mg/mL); y is a molar ratio of comonomer to AAm (mol %); z is the total monomer concentration of AAm and comonomer (w/v %). M is the abbreviation for various monomers, i.e., DMAAm for *N*,*N*′-dimethylacrylamide, DMAPMA for *N*-(3-dimethylaminopropyl)methacrylamide, HEAA for *N*-(2-hydroxyethyl)acrylamide, IMA for isodecyl methacrylate, LMA of lauryl methacrylate, and SMA of stearyl methacrylate. [b]The gels were synthesized with 0.03 mol % MBA. [c]The gels were prepared without MBA.

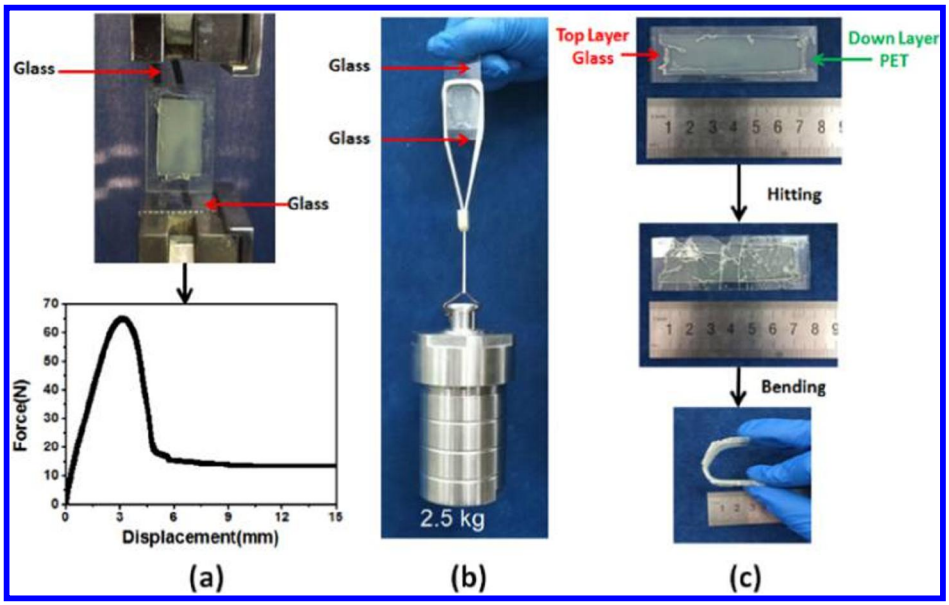

Figure 4. BSA/PAAm DN gels show strong adhesion on glass, allowing to (a) stick two glass slides, (b) lift a 2.5 kg weight, and (c) prevent broken glass pieces.

86/59% at 80 °C, respectively, all of which are much higher than 32/36% for the heat-untreated gel at room temperature (R.T.) (Figure 3b$_2$). Similarly, mechanical properties can be recovered with the increase of resting time. Particularly, after 30 min of resting at 80 °C, the stiffness/toughness recovery of the DN gel reached up to 94/80% (Figure 3C). Considering heating-induced protein denature is an irreversible process, such high self-recovery of the DN gels mainly stems from multiple, reversible physical interactions of hydrogen bonds and hydrophobic interactions between and within both networks, as well as dissociation of aggregated BSA proteins. As a counter example, BSA/PAAm semi-IPN gel showed a small mechanical hysteresis and almost no self-recovery (data not shown), indicating a lack of the aforementioned physical interactions. Taken together, the pronounced hysteresis and distinct yielding suggests significant energy dissipation upon stretching whereas the high self-recovery with heating temperature and resting time indicates that the BSA network reversibly breaks and reforms to toughen protein hydrogels via physical bonds (hydrogen bonds and hydrophobic interactions).

To prove that our fabrication method and protein–polymer system could be generally applicable to other BSA-based DN hydrogels, we used and polymerized *N*,*N*′-dimethylacrylamide (DMAAm), *N*-(3-dimethylaminopropyl)methacrylamide (DMAPMA), and *N*-(2-hydroxyethyl)acrylamide (HEAA) to construct a distinct second network interpenetrating with the BSA network (Scheme 1), producing BSA/PDMAAm, BSA/P(DMAPMA-*co*-AAm), and BSA/PHEAA DN hydrogels. Mechanical properties of these different BSA-based DN hydrogels are summarized in Table 1. BSA/PDMAAm DN gel and BSA/P(DMAPMA-*co*-AAm) DN gel, with the hybrid network structure similar to that of BSA/PAAm DN gel, also showed high tensile stress of ~0.3 MPa. BSA/PHEAA DN gel, as a fully physically linked DN gel without any chemical cross-linkers, also exhibited high tensile stress of 0.34 MPa similar to that of hybrid BSA-based DN hydrogels. Considering that BSA often serves as a carrier for hydrophobic molecules (e.g., lipophilic vitamins and hormones) in blood,[51] different hydrophobic comonomers, i.e., isodecyl methacrylate (IMA), lauryl methacrylate (LMA), and stearyl methacrylate (SMA), are readily dissolved in the BSA solution without the assistance of surfactants. So, fully physical BSA/P(IMA-*co*-AAm), BSA/

DOI: 10.1021/acs.chemmater.8b03860
Chem. Mater. 2019, 31, 179–189

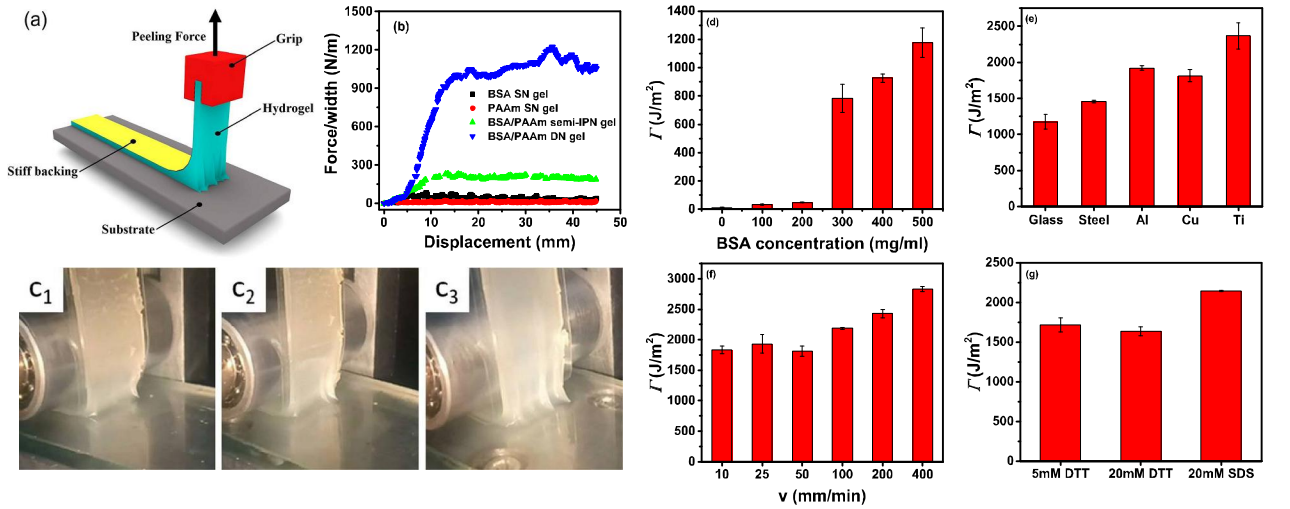

Figure 5. (a) Schematic diagram of the peeling test; (b) peeling-force–displacement curves for different hydrogels on glass; (c) visual inspection of peeling off BSA/PAAm DN gel from a glass substrate. The interfacial toughness of BSA/PAAm DN hydrogels as a function of (d) BSA concentrations, (e) different solid substrates, (f) peeling rates, and (g) other additives of dithiothreitol (DTT) and sodium dodecyl sulfate (SDS).

P(LMA-*co*-AAm), and BSA/P(SMA-*co*-AAm) DN gel can also be prepared in the absence of chemical cross-linkers and surfactant using the same synthesis procedure as that shown in Scheme 1. These BSA/P(I/L/SMA-*co*-AAm) gels demonstrated relatively lower tensile strength of ~0.25 MPa but much larger tensile strain of 72–80 mm/mm than that of BSA/PAAm DN gel. However, they may not recover their original length after unloading because the second component P(I/L/SMA-*co*-AAm) might flow during stretching. We also found that these gels displayed obvious necking during stretching. We reason that the interactions between BSA and hydrophobic monomers or BSA–monomer complexes are not strong enough to hold the integrity of the gel network after unloading. By virtue of this method, all of these BSA–polymer DN hydrogels reach high tensile stress of 0.24–0.48 MPa, tensile strain of 7.7–79.9 mm/mm, elastic modulus of 252–1199 kPa, and work of extension of 2.64–16.88 MJ/m^3. Besides BSA, we have also tested and demonstrated the heat-induced gelation behavior of different natural proteins, including human serum albumin, ovalbumin (OVA), β-lactoglobulin, and soy protein. Among them, only OVA/PDMAAm DN gel has been successfully synthesized but with low mechanical properties, which could be caused by poor mechanical strength of OVA network and unoptimized polymerization conditions (e.g., low concentration of OVA) (Table 1). We still believe that careful modification of this one-pot method and proper selection of natural proteins with good water solubility are the keys to design and fabricate new and tough protein–polymer DN hydrogels, as well as to expand the general applicability for a wide variety of protein–polymer combinations.

More interestingly, our BSA/PAAm DN gels also showed strong adhesion to various nonporous solids without any surface modification. The hydrogel–solid bonding interface can be formed by the direct fabrication of BSA/PAAm DN gels on the nonporous solid surface via the same preparation process as that described in Scheme 1. After in situ polymerization, two glass slides bonded by BSA/PAAm DN gel with a small contact area of 18 × 25 × 1 mm^3 enabled to bear a shear force up to ~65 N (i.e., shear strength of 3.6 MPa) (Figure 4a) and to lift a 2.5 kg weight (Figure 4b). Moreover, the strong adhesion of BSA/PAAm DN gel between a glass slide and a poly(ethylene terephthalate) (PET) film not only prevented broken glass pieces from splashing around when hitting the glass slide but also allowed the "sandwich-like" sample to bend over without the detachment of glass pieces (Figure 4c).

The adhesive energy of BSA/PAAm DN gels on a nonporous glass was quantitatively examined by the 90° peeling test at the peeling rate of 50 mm/min (Figure 5a and Table S7). There was no chemical modification on the glass for promoting the interfacial bonding between the gel and the glass surface. The peeling-force–displacement curves showed that BSA/PAAm DN gel strongly adhered on the glass surface and achieved high interfacial toughness of 1176 J/m^2, which was 5.9, 26.7, and 98 times higher than that of BSA/PAAm semi-IPN gel (200 J/m^2), BSA SN gel (44 J/m^2), and PAAm SN gel (12 J/m^2) (Figure 5b). The finger pattern with increasing amplitude was also observed at the gel–glass interface (Figure 5c). The interfacial toughness of BSA SN gel on glass (44 J/m^2) was much larger than that of PAAm SN gel (12 J/m^2) and chemically anchored PAAm SN gel on the glass (24 J/m^2) in the literature,[41] indicating the intrinsic adhesion of BSA SN gel on glass. The peeling process of BSA SN gel, PAAm SN gel, and BSA/PAAm semi-IPN gel is shown in Figure S3.

We further examined the effects of C_{BSA}, solid substrates, peeling rates, and other additives on the interfacial toughness of BSA/PAAm DN gels. As shown in Figure 5d and Table S8, the interfacial toughness of BSA/PAAm DN gels monotonously increased from 12 to 1176 J/m^2 as C_{BSA} increased from 0 to 500 mg/mL. The increase of interfacial toughness with C_{BSA} was consistent with the increase of bulk toughness with C_{BSA}, indicating that the strong hydrogel–solid interface generally requires high fracture toughness of the hydrogel itself to ensure that the adhesion failure occurs at the gel–solid interface, not in the body of the gel. More importantly, BSA/PAAm DN gel has also demonstrated its strong adhesion to different nonporous substrates without any surface modification (Figure 5e and Table S9). The measured interfacial toughness of the gels was 1460 J/m^2 on steel, 1920 J/m^2 on Al, 1812 J/m^2 on Cu, and 2366 J/m^2 on Ti, respectively. All gel–

DOI: 10.1021/acs.chemmater.8b03860
Chem. Mater. 2019, 31, 179–189

solid systems consistently showed high interfacial toughness, proving that our design strategy and fabrication method are generally applicable to generate tough bonding of protein-based hydrogels to different solids. We further varied the peeling rate from 10 to 400 mm/min, and the measured interfacial toughness of BSA/PAAm DN gel on Cu increased from 1834 to 2827 J/m^2 (Figure 5f and Table S10). The rate dependence of interfacial toughness is likely attributed to the viscoelasticity of the BSA/PAAm DN gels, which is correlated with the rate-dependent energy dissipation behavior (Figure S2b). To further understand the interfacial interactions between the gel and solid surface, we introduced dithiothreitol (DTT) and sodium dodecyl sulfate (SDS) to disrupt the interactions between BSA gels and solid surface, because DTT is a reductant for disulfide group and SDS is a denaturant for BSA. In Figure 5g and Table S11, interfacial toughness of DN gels decreased slightly with DTT concentration, indicating that disulfide groups in BSA could interact with Cu so that more free −SH groups enable to reduce the mechanical properties of bulk DN gels due to chain-transfer effect. A small amount of SDS (20 mM) largely improved the bonding of the gel on copper from 1812 to 2142 J/m^2, probably because SDS induces further unfolding of BSA proteins and exposes more groups to enhance interaction with metal surface. The heat-induced denaturing and unfolding of BSA on the substrate is fundamentally different from those of BSA in bulk solution, because many studies have reported that the presence of substrates has a strong influence on protein conformation and activity. Thus, application of preprepared BSA/PAAm DN gels onto substrates just did not result in adherence onto the substrates. The high interfacial toughness (Γ) of BSA/PAAm DN gels to various solid substrates is the sum of two parts, i.e., intrinsic adhesive energy of BSA SN gel on solid substrates (Γ_0) and adhesive energy caused by large dissipated energy of BSA/PAAm DN gels (Γ_d). Therefore, $\Gamma = \Gamma_0 + \Gamma_d$.[41] As shown in Figures 5b and S4, BSA SN gel exhibited Γ_0 of 44 and 25 J/m^2 on glass and Ti, respectively, indicating there is intrinsic adhesion of BSA SN gel on them. Meanwhile, the large hysteresis loop of BSA/PAAm DN gels is also observed in Figure 3a. The intrinsic adhesion of BSA SN gel on various substrates will maintain cohesion of the gel−solid interface, allowing large deformation and effective energy dissipation in bulk DN gels to generate high values of Γ_d. Consequently, our BSA/PAAm DN gels exhibited tough adhesion on various substrates. It should be noted that we have also tested the interfacial toughness of BSA/PAAm hydrogels upon swelling in water for 1 h. However, interfacial toughness of BSA/PAAm DN hydrogels was only 24 J/m^2 so that the gels can be easily peeled off from the glass, indicating that the physical nature of interfacial bonding (e.g., hydrogen bonds) is largely disrupted in water due to the swelling-induced network expansion and weakness. Taken together, BSA-based DN gels not only demonstrated highly mechanical properties but also exhibited high interfacial toughness on various nonporous solid substrates without any surface modification. From Figure 6a, our BSA-based DN gels show much better tensile properties compared to those of other natural protein-based hydrogels. Figure 6b also shows that the interfacial toughness of BSA/PAAm DN gel was comparable to that of chemically anchored alginate/PAAm hybrid gels (1000−1750 J/m^2),[41] interfacial bridged alginate/PAAm hybrid gels (~1000 J/m^2),[32] cyanoacrylate glued alginate/PAAm hybrid gels (1427 J/m^2), poly(vinyl alcohol) gel (2208 J/m^2),[52] and agar/PHEAA gel (2000−5600 J/m^2).[43] The high interfacial toughness of BSA/PAAm DN gel is attributed to large energy dissipation in bulk hydrogels and strong interaction between gel and solids.

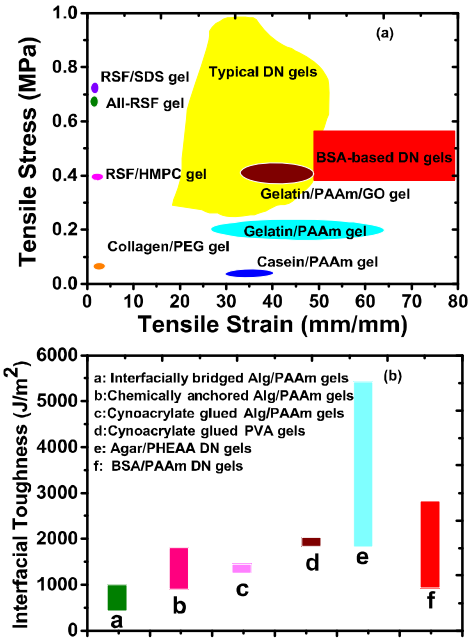

Figure 6. Comparison of tensile stress−strain between BSA-based DN gels and other natural protein-based hydrogels; (b) comparison of interfacial toughness between BSA/PAAm DN gels and other hydrogels on various substrates.

3. CONCLUSIONS

In summary, we demonstrate a simple yet general strategy to fabricate strong globular protein−synthetic polymer hydrogels with both excellent mechanical properties and surface adhesion via the "double network" and "protein misfolding" principles. This new strategy uses the intrinsic heat-induced denaturation, aggregation, and gelation of BSA proteins to construct a common sacrificial protein network for energy dissipation, in combination with a distinct second polymer network (covalently or physically cross-linked), to produce different BSA-based DN hydrogels. The BSA-based DN hydrogels demonstrate not only highly mechanical properties (tensile stress of 0.24−0.48 MPa, tensile strain of 7.7−79.9 mm/mm, tensile modulus of 252−1199 kPa, work of extension of 3.56−16.88 MJ/m^3, and compressive stress of 50 MPa), large hysteresis, and self-recovery properties (stiffness/toughness recovery of 94/80% after heat treatment at 80 °C for 30 min) but also strong and robust interfacial bonding to different nonporous solids without any surface modification (interfacial toughness of 1176−2827 J/m^2). This work introduces a new gel system to harness distinctive yet complementary advantages of proteins and polymers for developing hybrid protein−polymer hydrogels and exploring different applications.

4. EXPERIMENTAL SECTION

4.1. Materials. Bovine serum albumin (BSA, 98%) and ovalbumin (OVA, albumin from chicken egg white, 62−88%) were purchased from Sigma-Aldrich Inc. Acrylamide (AAm, 98%), 2-hydroxy-4′-(2-hydroxyethoxy)-2-methylpropiophenone (Irgacure 2959), *N*,*N*-dimethylacrylamide (DMAAm, >99.0%), and *N*-(2-hydroxyethyl)-acrylamide (HEAA, >98.0%) were purchased from TCI Shanghai

DOI: 10.1021/acs.chemmater.8b03860
Chem. Mater. 2019, 31, 179−189

Inc. *N*-[3-(Dimethylamino)propyl]methacrylamide (DMAPMA, 98%), isodecyl methacrylate (IMA, 95%), lauryl methacrylate (LMA, 96%), stearyl methacrylate (SMA, 96%), and *N*,*N*′-methylenebis(acrylamide) (MBA, 99%) were purchased from Aladdin (Shanghai) Inc. All materials were used without further purification.

4.2. Synthesis of Hydrogels. BSA/PAAm DN hydrogels were synthesized by the one-pot method as reported in our previous work with some modifications. Briefly, BSA (4 g, 500 mg/mL), AAm (2.4 g, 30% w/v), 2-hydroxy-4′-(2-hydroxyethoxy)-2-methylpropiophenone (0.0757 g, Irgacure 2959, 1 mol % of AAm), and *N*,*N*′-methylenebisacrylamide solution (59 μL, 0.03 mol % of AAm, MBA solution was 20 mg/mL) were dissolved into H_2O (8 mL) in a reactor. After degassing three times, the reactor was sealed under N_2 protection. Then, the obtained precursor solution was injected into a cylindrical plastic mold (D = 8.5 mm), followed by a heating procedure at 80 °C for 10 min in a water bath to form the BSA network. Upon cooling down to room temperature, AAm monomers inside the BSA network were then photopolymerized by UV light (365 nm wavelength, 8 W) for 1 h to form the PAAm network, interpenetrating with the BSA network to produce BSA/PAAm DN gel. The resultant BSA/PAAm gels were stored at 4 °C for mechanical tests.

The same method was used to synthesize BSA/PAAm gel on a solid substrate for peeling tests, except that the precursor solution was injected into a mold consisting of a glass slide covered with PET film, a Teflon spacer (thickness of 1 mm), and a rigid substrate or another glass slide covered with PET film. Prior to hydrogel synthesis on the substrate, the substrate was cleaned with 30 min of sonication in acetone, ethanol, and water sequentially and completely dried.

The BSA/PDMAAm DN gel, OVA/PDMAAm DN gel, and BSA/P(DMAPMA-*co*-AAm) gel were synthesized by the same method. The BSA/P(IMA-*co*-AAm), BSA/P(LMA-*co*-AAm), BSA/P(SMA-*co*-AAm), and BSA/PHEAAm DN gels were synthesized by similar methods except for no cross-linker agent used. BSA SN hydrogels, PAAm SN hydrogels, and BSA/PAAm semi-IPN gels were prepared using the modified one-pot method. BSA SN gels were directly synthesized through the heating process without involving photopolymerization. PAAm SN hydrogels and BSA/PAAm semi-IPN gels were directly synthesized through the photopolymerization process. All gels were used at the as-prepared state, not at a swollen state, for mechanical tests. We have examined the swelling properties of BSA SN gel and BSA/PAAm DN gel. The swelling ratio of the gels was evaluated by m/m_0, where m is the weight of the swollen gel after swelling for 24 h in aqueous solution at room temperature and m_0 is the weight of as-prepared gel. Interestingly, we found that BSA SN gel almost did not swell and its size did not change much after 24 h of immersion. The swelling ratio of BSA SN gel was 1.2. However, BSA/PAAm DN gel clearly showed a swelling behavior, as indicated by the increase of gel size and a swelling ratio of 4.3. This result suggests that the swelling of BSA/PAAm DN gel was mainly dominated by the PAAm network. Therefore, the swelling of BSA/PAAm DN gel was balanced by the competition between the "low-swollen" BSA network and the "highly swollen" PAAm network.

4.3. Mechanical Test of Hydrogels. Compression and tensile tests were carried out with a WSM-10 kN machine. For compression tests, the cylindrical gel samples with 8.5 mm diameter were cut into 10 mm height pieces, the compress strain was estimated as h/h_0, where h is the deformed height and h_0 is the original height. The compression stress was measured as F/A_0, where F is the force applied on the gel and A_0 is the original cross-sectional area of the gel sample. The compression rate was 5 mm/min. The cylindrical gel samples with 8.5 mm diameter were directly used for tensile tests. The nominal tensile strain (ε) was defined as the change in the length (Δl) divided by the original length (l_0) of the specimen ($\varepsilon = \Delta l/l_0$). The nominal stress ($\sigma$) was obtained by dividing the force (F') by the original cross-sectional area (A_0') of the specimen ($\sigma = F'/A_0'$). The tensile rate was 100 mm/min.

The hysteresis tests of gels were also conducted by the above tensile tester. Gel samples were stretched by a loading cycle to different maximum elongation ratios (λ_{max}, $\lambda = \varepsilon + 1$), with a loading–unloading rate of 100 mm/min, or by a loading cycle to a maximum elongation ratio of λ_{max} = 8 with different loading–unloading rates. For recovery experiments, the samples were first stretched by a loading–unloading cycle to achieve a maximum elongation ratio (λ_{max} = 8) and then the samples were sealed in the plastic ziplock bag and stored at 40, 60, and 80 °C or at room temperature for 0, 5, 10, 20, and 30 min. Then, the samples were taken out and cooled down at room temperatures prior to tests.

The interfacial toughness between the hydrogel and the solid substrates was measured via 90° peeling tests using the same tensile tester with a different down grip. After the substrate adhesive with hydrogel was fixed on the down grip, the gel samples covered with PET stiff backing were tested with a standard 90° peeling test setup (Figure 5a).

4.4. Characterization. Morphologies of hydrogel samples were obtained by a field emission scanning electron microscope (Merlin Compact, Zeiss) at an acceleration voltage of 15 kV. All gel samples were frozen and fractured in liquid nitrogen and dried in a lyophilizer. Before tests, the samples were coated with a thin layer of gold.

■ ASSOCIATED CONTENT

Supporting Information

The Supporting Information is available free of charge on the ACS Publications website at DOI: 10.1021/acs.chemmater.8b03860.

Effects of different network components, heating temperature, and heating time on mechanical properties; hysteresis tests and adhesive tests (PDF)

■ AUTHOR INFORMATION

Corresponding Authors

*E-mail: chenqiang@hpu.edu.cn (Q.C.).
*E-mail: zhengj@uakron.edu (J.Z.).

ORCID

Qiang Chen: 0000-0002-8592-9518
Jie Zheng: 0000-0003-1547-3612

Notes

The authors declare no competing financial interest.

■ ACKNOWLEDGMENTS

Q.C. is grateful for financial support, in part, from National Nature Science Foundation of China (21504022), the Joint Fund for Fostering Talents of NSFC-Henan Province (U1304516), Henan Province (NSFRF1605, 2016GGJS-039, and 17HASTIT006), and Henan Polytechnic University (72105/001 and 672517/005). J.Z. acknowledges financial support from NSF grants (DMR-1607475 and CMMI-1825122).

■ REFERENCES

(1) Lee, K. Y.; Mooney, D. J. Hydrogels for Tissue Engineering. *Chem. Rev.* **2001**, *101*, 1869–1879.
(2) Tibbitt, M. W.; Langer, R. Living Biomaterials. *Acc. Chem. Res.* **2017**, *50*, 508–513.
(3) Wang, W.; Zhang, Y.; Liu, W. Bioinspired fabrication of high strength hydrogels from non-covalent interactions. *Prog. Polym. Sci.* **2017**, *71*, 1–25.
(4) Gomes, S.; Leonor, I. B.; Mano, J. F.; Reis, R. L.; Kaplan, D. L. Natural and genetically engineered proteins for tissue engineering. *Prog. Polym. Sci.* **2012**, *37*, 1–17.
(5) Yang, C.; Suo, Z. Hydrogel ionotronics. *Nat. Rev. Mater.* **2018**, *3*, 125–142.
(6) Hoare, T.; Kohane, D. S. Hydrogels in drug delivery: Progress and challenges. *Polymer* **2008**, *49*, 1993–2007.

DOI: 10.1021/acs.chemmater.8b03860
Chem. Mater. 2019, 31, 179–189

(7) Taylor, D. L.; In, H. P. M. Self-Healing Hydrogels. *Adv. Mater.* **2016**, *28*, 9060−9093.
(8) Zhao, X. Multi-scale multi-mechanism design of tough hydrogels: building dissipation into stretchy networks. *Soft Matter* **2014**, *10*, 672−687.
(9) Zhao, X. Designing toughness and strength for soft materials. *Proc. Natl. Acad. Sci.* **2017**, *114*, 8138−8140.
(10) Tan, C. S. Y.; Liu, J.; Groombridge, A. S.; Barrow, S. J.; Dreiss, C. A.; Scherman, O. A. Controlling Spatiotemporal Mechanics of Supramolecular Hydrogel Networks with Highly Branched Cucurbit [8] uril Polyrotaxanes. *Adv. Funct. Mater.* **2018**, *28*, No. 1702994.
(11) Silva, N.; Vilela, C.; Marrucho, I. M.; Freire, C. S. R.; Neto, C. P.; Silvestre, A. J. D. Protein-based materials: from sources to innovative sustainable materials for biomedical applications. *J. Mater. Chem. B* **2014**, *2*, 3715−3740.
(12) Jonker, A. M.; Lowik, D. W. P. M.; Van Hest, J. C. M. Peptide- and Protein-Based Hydrogels. *Chem. Mater.* **2012**, *24*, 759−773.
(13) Gong, J. P. Materials both Tough and Soft. *Science* **2014**, *344*, 161−162.
(14) Van Vlierberghe, S.; Dubruel, P.; Schacht, E. Biopolymer-Based Hydrogels As Scaffolds for Tissue Engineering Applications: A Review. *Biomacromolecules* **2011**, *12*, 1387−1408.
(15) Kapoor, S.; Kundu, S. C. Silk protein-based hydrogels: Promising advanced materials for biomedical applications. *Acta Biomater.* **2016**, *31*, 17−32.
(16) Ni, N.; Dumont, M. Protein-Based Hydrogels Derived from Industrial Byproducts Containing Collagen, Keratin, Zein and Soy. *Waste Biomass Valorization* **2017**, *8*, 285−300.
(17) Sun, Y.; Huang, Y. Disulfide-crosslinked albumin hydrogels. *J. Mater. Chem. B* **2016**, *4*, 2768−2775.
(18) Le, X. T.; Rioux, L.; Turgeon, S. L. Formation and functional properties of protein−polysaccharide electrostatic hydrogels in comparison to protein or polysaccharide hydrogels. *Adv. Colloid Interface Sci.* **2017**, *239*, 127−135.
(19) Mehrali, M.; Thakur, A.; Pennisi, C. P.; Talebian, S.; Arpanaei, A.; Nikkhah, M.; Dolatshahipirouz, A. Nanoreinforced Hydrogels for Tissue Engineering: Biomaterials that are Compatible with Load-Bearing and Electroactive Tissues. *Adv. Mater.* **2017**, *29*, No. 1603612.
(20) Zhang, Y. S.; Khademhosseini, A. Advances in engineering hydrogels. *Science* **2017**, *356*, No. eaaf3627.
(21) Gaharwar, A. K.; Avery, R. K.; Assmann, A.; Paul, A.; Mckinley, G. H.; Khademhosseini, A.; Olsen, B. D. Shear-thinning nanocomposite hydrogels for the treatment of hemorrhage. *ACS Nano* **2014**, *8*, 9833−9842.
(22) Xavier, J. R.; Thakur, T.; Desai, P.; Jaiswal, M. K.; Sears, N.; Cosgriffhernandez, E.; Kaunas, R.; Gaharwar, A. K. Bioactive Nanoengineered Hydrogels for Bone Tissue Engineering: A Growth-Factor-Free Approach. *ACS Nano* **2015**, *9*, 3109−3118.
(23) Shin, S. R.; Zihlmann, C.; Akbari, M.; Assawes, P.; Cheung, L.; Zhang, K.; Manoharan, V.; Zhang, Y. S.; Yüksekkaya, M.; Wan, K.-t.; et al. Reduced graphene oxide-gelMA hybrid hydrogels as scaffolds for cardiac tissue engineering. *Small* **2016**, *12*, 3677−3689.
(24) Yetiskin, B.; Akinci, C.; Okay, O. Cryogelation within cryogels: Silk fibroin scaffolds with single-, double-and triple-network structures. *Polymer* **2017**, *128*, 47−56.
(25) Li, Z.; Zheng, Z.; Yang, Y.; Fang, G.; Yao, J.; Shao, Z.; Chen, X. Robust protein hydrogels from silkworm silk. *ACS Sustainable Chem. Eng.* **2016**, *4*, 1500−1506.
(26) Luo, K.; Yang, Y.; Shao, Z. Physically Crosslinked Biocompatible Silk-Fibroin-Based Hydrogels with High Mechanical Performance. *Adv. Funct. Mater.* **2016**, *26*, 872−880.
(27) Chan, B. K.; Wippich, C. C.; Wu, C. J.; Sivasankar, P. M.; Schmidt, G. Robust and Semi-Interpenetrating Hydrogels from Poly(ethylene glycol) and Collagen for Elastomeric Tissue Scaffolds. *Macromol. Biosci.* **2012**, *12*, 1490−1501.
(28) Ma, J.; Lee, J.; Han, S. S.; Oh, K. H.; Nam, K. T.; Sun, J.-Y. Highly stretchable and notch-insensitive hydrogel based on polyacrylamide and milk protein. *ACS Appl. Mater. Interfaces* **2016**, *8*, 29220−29226.
(29) Zhao, Y.; Wu, Y.; Wang, L.; Zhang, M.; Chen, X.; Liu, M.; Fan, J.; Liu, J.; Zhou, F.; Wang, Z. Bio-inspired reversible underwater adhesive. *Nat. Commun.* **2017**, *8*, No. 2218.
(30) Yang, J.; Bai, R.; Suo, Z. Topological adhesion of wet materials. *Adv. Mater.* **2018**, *30*, No. 1800671.
(31) Liang, S.; Zhang, Y.; Wang, H.; Xu, Z.; Chen, J.; Bao, R.; Tan, B.; Cui, Y.; Fan, G.; Wang, W.; et al. Paintable and Rapidly Bondable Conductive Hydrogels as Therapeutic Cardiac Patches. *Adv. Mater.* **2018**, *30*, No. 1704235.
(32) Li, J.; Celiz, A.; Yang, J.; Yang, Q.; Wamala, I.; Whyte, W.; Seo, B.; Vasilyev, N.; Vlassak, J.; Suo, Z. Tough adhesives for diverse wet surfaces. *Science* **2017**, *357*, 378−381.
(33) Bouten, P. J.; Zonjee, M.; Bender, J.; Yauw, S. T.; van Goor, H.; van Hest, J. C.; Hoogenboom, R. The chemistry of tissue adhesive materials. *Prog. Polym. Sci.* **2014**, *39*, 1375−1405.
(34) Liu, X.; Zhang, Q.; Gao, G. Bioinspired Adhesive Hydrogels Tackified by Nucleobases. *Adv. Funct. Mater.* **2017**, *27*, No. 1703132.
(35) Han, L.; Lu, X.; Liu, K.; Wang, K.; Fang, L.; Weng, L.-T.; Zhang, H.; Tang, Y.; Ren, F.; Zhao, C.; et al. Mussel-inspired adhesive and tough hydrogel based on nanoclay confined dopamine polymerization. *ACS Nano* **2017**, *11*, 2561−2574.
(36) Xu, J.; Fan, Z.; Duan, L.; Gao, G. A tough, stretchable, and extensively sticky hydrogel driven by milk protein. *Polym. Chem.* **2018**, *9*, 2617−2624.
(37) Liu, Q.; Nian, G.; Yang, C.; Qu, S.; Suo, Z. Bonding dissimilar polymer networks in various manufacturing processes. *Nat. Commun.* **2018**, *9*, No. 846.
(38) Han, L.; Liu, K.; Wang, M.; Wang, K.; Fang, L.; Chen, H.; Zhou, J.; Lu, X. Mussel-Inspired Adhesive and Conductive Hydrogel with Long-Lasting Moisture and Extreme Temperature Tolerance. *Adv. Funct. Mater.* **2018**, *28*, No. 1704195.
(39) Liu, J.; Scherman, O. A. Cucurbit[n]uril Supramolecular Hydrogel Networks as Tough and Healable Adhesives. *Adv. Funct. Mater.* **2018**, *28*, No. 1800848.
(40) Kurokawa, T.; Furukawa, H.; Wang, W.; Tanaka, Y.; Gong, J. P. Formation of a strong hydrogel−porous solid interface via the double-network principle. *Acta Biomater.* **2010**, *6*, 1353−1359.
(41) Yuk, H.; Zhang, T.; Lin, S.; Parada, G. A.; Zhao, X. Tough bonding of hydrogels to diverse non-porous surfaces. *Nat. Mater.* **2016**, *15*, 190.
(42) Yuk, H.; Zhang, T.; Parada, G. A.; Liu, X.; Zhao, X. Skin-inspired hydrogel−elastomer hybrids with robust interfaces and functional microstructures. *Nat. Commun.* **2016**, *7*, No. 12028.
(43) Chen, H.; Liu, Y.; Ren, B.; Zhang, Y.; Ma, J.; Xu, L.; Chen, Q.; Zheng, J. Super Bulk and Interfacial Toughness of Physically Crosslinked Double-Network Hydrogels. *Adv. Funct. Mater.* **2017**, *27*, No. 1703086.
(44) Yan, X.; Chen, Q.; Zhu, L.; Chen, H.; Wei, D.; Chen, F.; Tang, Z.; Yang, J.; Zheng, J. High strength and self-healable gelatin/polyacrylamide double network hydrogels. *J. Mater. Chem. B* **2017**, *5*, 7683−7691.
(45) Huang, J.; Zhao, L.; Wang, T.; Sun, W.; Tong, Z. Nir-triggered rapid shape memory PAM−GO−gelatin hydrogels with high mechanical strength. *ACS Appl. Mater. Interfaces* **2016**, *8*, 12384−12392.
(46) Gong, J. P.; Katsuyama, Y.; Kurokawa, T.; Osada, Y. Double-network hydrogels with extremely high mechanical strength. *Adv. Mater.* **2003**, *15*, 1155−1158.
(47) Chen, J.; Ma, X.; Dong, Q.; Song, D.; Hargrove, D.; Vora, S. R.; Ma, A. W.; Lu, X.; Lei, Y. Self-healing of thermally-induced, biocompatible and biodegradable protein hydrogel. *RSC Adv.* **2016**, *6*, 56183−56192.
(48) Chen, J.; Dong, Q.; Ma, X.; Fan, T.-H.; Lei, Y. Repetitive Biomimetic Self-healing of Ca^{2+}-Induced Nanocomposite Protein Hydrogels. *Sci. Rep.* **2016**, *6*, No. 30804.

DOI: 10.1021/acs.chemmater.8b03860
Chem. Mater. 2019, 31, 179−189

(49) Durand, D.; Gimel, J. C.; Nicolai, T. Aggregation, gelation and phase separation of heat denatured globular proteins. *Phys. A* **2002**, *304*, 253−265.
(50) Clark, A.; Kavanagh, G.; Ross-Murphy, S. Globular protein gelation—theory and experiment. *Food Hydrocolloids* **2001**, *15*, 383−400.
(51) Chen, Q.; Liu, Z. Albumin carriers for cancer theranostics: a conventional platform with new promise. *Adv. Mater.* **2016**, *28*, 10557−10566.
(52) Wirthl, D.; Pichler, R.; Drack, M.; Kettlguber, G.; Moser, R.; Gerstmayr, R.; Hartmann, F.; Bradt, E.; Kaltseis, R.; Siket, C. M.; et al. Instant tough bonding of hydrogels for soft machines and electronics. *Sci. Adv.* **2017**, *3*, No. e1700053.

DOI: 10.1021/acs.chemmater.8b03860
Chem. Mater. 2019, 31, 179−189